Check for updates

Investigation on the enhanced catalytic activity of a Ni-promoted Pd/C catalyst for formic acid dehydrogenation: effects of preparation methods and Ni/Pd ratios†

Yongwoo Kim, Jonghyun Kim and Do Heui Kim [ID] *

In this present work, we studied the effects of preparation methods and Ni/Pd ratios on the catalytic activity of a Ni-promoted Pd/C catalyst for the formic acid dehydrogenation (FAD) reaction. Two catalysts prepared by co-impregnation and sequential impregnation methods showed completely different Pd states and catalytic activities. As the sequentially impregnated catalyst showed better activity than the co-impregnated catalyst, the sequentially impregnated catalyst was investigated further to optimize the ratio of Ni/Pd. The highest catalytic activity for the FAD reaction was obtained over the seq-impregnated catalyst having a 1 : 1.3 molar ratio of Pd : Ni. The results of X-ray diffraction (XRD) and transmission electron microscopy (TEM) showed that small particle size is one factor improving the catalytic activity, while those of X-ray photoelectron spectroscopy (XPS) and X-ray adsorption near edge structure (XANES) indicate that the electronic modification of Pd to a positively charged ion is another factor. Thus, it can be concluded that the enhanced catalytic activity of the Ni-promoted Pd/C catalyst is attributed to the role of pre-impregnated Ni in facilitating the activity of Pd by constraining the particle growth and withdrawing an electron from Pd.

Introduction

Fossil fuel, which currently provides the largest source of energy, will not only be depleted in the near future but also causes lots of environmental problems.[1,2] Thus, one of the ultimate goals that should be achieved is to find a sustainable energy source having no detrimental effect on the environment. In this respect, hydrogen is considered to be a future energy carrier due to its reusability, high energy density and eco-friendly properties.[3] Although the uses of hydrogen have been widely known in various fields, there are storage problems arising from its flammability and difficulty in conveyance.[4–6] Many researchers have investigated methods to store and transport hydrogen resource safely.[7–9] One possible solution is to use hydrogen-containing material to carry hydrogen. Formic acid (FA) has received attention as a hydrogen source, since FA can be decomposed into H_2 and CO_2 at mild temperature. Furthermore, as FA is a non-toxic and free-carbon-stacking liquid material, the problems originating from hydrogen can

be solved without any side effects by adopting FA as a hydrogen storage media.[10,11]

In order to decompose FA into H_2 and CO_2 under ambient condition, the catalyst should be utilized during the reaction. Pd has been known as the most active metal for aqueous formic acid dehydrogenation (FAD) reaction.[12,13] However, Pd/C is inadequate catalyst for commercial application, because it has insufficient activity and even generates carbon monoxide (CO) via dehydration of FA which can poison catalysts in fuel cell.[14–16] Therefore, it is inevitable to develop a new catalyst which has enhanced activity and high H_2 selectivity. Previous researches have tried to improve the catalytic activity, selectivity and reusability of Pd-based catalyst by modifying supports, adding various promoters or optimizing reactant with sodium formate.[14,15,17–26] Herein, in a way to improve the FAD catalytic activity, we applied two preparation methods to synthesize bimetallic catalysts; co-impregnation and sequential impregnation (i.e. seq-impregnation) methods which are simply depicted in Fig. 1. The former is to impregnate Pd and promoting metal on carbon simultaneously. The latter is to impregnate the promoting metal on carbon first, followed by impregnating Pd on metal/C. Since some transition metals can be easily oxidized to metal oxide even under mild oxidative condition such as drying condition in synthetic process, the interaction between the metal and Pd of co-impregnated catalyst was expected to be totally different from that between the

School of Chemical and Biological Engineering, Institute of Chemical Processes, Seoul National University, 1 Gwanak-ro, Gwanak-gu, Seoul 151-742, Korea. E-mail: dohkim@snu.ac.kr
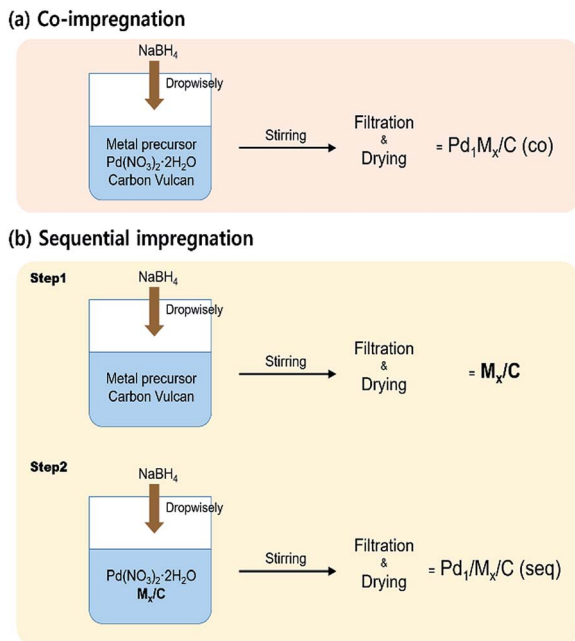
Fig. 1 Schematic diagram of preparation processes of (a) co-impregnated and (b) seq-impregnated catalysts.

metal oxide and Pd of seq-impregnated catalyst if metal oxide is formed before impregnation of Pd. The catalysts prepared by co-impregnation and seq-impregnation methods are designated as Pd_1M_x/C (co) and $Pd_1/M_x/C$ (seq), respectively, both of which are composed of x molar ratio of metal/Pd based on ICP-AES result. The content of Pd is fixed at almost same value ($\sim$9 wt%) in all catalysts.

Several bimetallic Pd-M/C (M = Fe, Co, Ni, Cu, Zn and Ag) catalysts were prepared by applying two different methods to screen proper promoter. The result showed that Co, Ni, and Ag have promoting effect. Among them, $Pd_1/NiO_{0.9}/C$ (seq) has the highest activity (Fig. S1†). It is also worth to note that the promoting effect is generally higher over the seq-impregnated catalyst than the co-impregnated catalyst. Although the promoting effects of Co, Ni and Ag have already been reported, to the best of our knowledge, no attempt has been made to prepare FAD catalyst by seq-impregnation method.[21,27,28] Although none of monometallic catalyst except Pd shows any catalytic activity for FAD reaction (Fig. S1†), De et al. variously showed the role of Ni in inducing the modification of surface properties of bimetallic catalysts.[29] Thus, the role of Ni in FAD reaction is considered to promote Pd to be more active rather than having catalytic activity by itself. The present work aimed at investigating the characteristics of various Ni-promoted Pd/C catalysts to identify the reasons for the enhanced activity by focusing especially on the changes of Pd state induced by Ni. Understanding the correlation between the activity and the state of Pd provided us with the information about the active Pd for FAD reaction, which can suggest a concrete direction to develop more advanced Pd-based FAD catalyst.

Experimental section

Catalysts preparation

All the catalysts were prepared by applying the chemical reduction method using $NaBH_4$ as a reductant. The preparation processes are simply depicted as diagram in Fig. 1.

Preparation of co-impregnated catalysts (Pd_1M_x/C (co))

Both target amounts of $Pd(NO_3)_2 \cdot 2H_2O$ (Sigma Aldrich) and metal precursors (Sigma Aldrich or Alfa Aesar) were dissolved together in the 40 mL distilled water with Vulcan XC72 (Cabot Co.). The solution was stirred for 2 h at high speed and subsequently sonicated for 1 h to disperse whole materials uniformly. Then, as-prepared $NaBH_4$ solution (10 times of moles of metal precursors) in the 45 mL distilled water was introduced to the solution dropwise for 45 min (1 mL min^{-1}) to reduce the metal precursors to the metals under vigorous stirring. After adding $NaBH_4$ solution, stirring process was carried out for 2 h. Thereafter, the catalyst was filtered and washed by the distilled water several times to get rid of residual ions of the precursors. Finally, the catalyst was dried at 100 °C in air overnight.

Preparation of seq-impregnated catalysts ($Pd_1/M_x/C$ (seq))

The process of preparing the seq-impregnated catalyst is quite similar with that of the co-impregnated catalyst. However, for the first step, the only target amount of metal precursor was dissolved in the 40 mL distilled water with Vulcan XC72. After the stirring and sonication processes to mix the solution, $NaBH_4$ solution was added. With the additional stirring period for reduction, the sample was filtered and dried at 100 °C in air overnight. In second step, after M_x/C was obtained, calculated amount of $Pd(NO_3)_2 \cdot 2H_2O$ was dissolved in the 40 mL distilled water with dried M_x/C. Once again the same processes (i.e. stirring, sonication, Pd^{2+} reduction by $NaBH_4$, filtration and drying) were carried out.

Preparation of monometallic catalysts (Pd/C, M/C)

The same synthetic process was performed to prepare Pd/C and M/C samples. In short, each metal precursor and Vulcan XC72 was dissolved in the distilled water. After the stirring and sonication processes for mixing the solution, $NaBH_4$ solution was added. With the additional stirring period, the catalyst was filtered and dried at 100 °C in air overnight.

Catalysts characterization

Inductively coupled plasma atomic emission spectroscopy (ICP-AES) was performed to determine the content of metals (i.e. Pd and Ni) in the catalysts by the ICPS-7500 (SHIMADZU). Before ICP-AES analysis, all the catalysts were pretreated in the mixture solution of $HCl : HNO_3$ (3 : 1 volumetric ratio) for 3 h at 95 °C. Then, after Vulcan XC72 in the solution was filtered by syringe filter, the solution was analyzed. X-ray diffraction (XRD) patterns were taken by using X-ray diffractometer (Rigaku) with Cu Kα radiation of X-ray current at 30 mA and generating voltage at 40 kV. The measurement regions were from 10 to 90°

with scan speed of 1.0 degree per min and scanning step size of 0.2° for high resolution. The particles in the catalysts were examined by transmission electron microscope (TEM) images, which were captured by JEM-2100F Transmission electron microscope (TEM, JEOL., Japan) with accelerating voltage of 200 kV. To identify the chemical state of Pd, X-ray photoelectron spectroscopy (XPS) was applied in the region of Pd 3d and Ni 2p with an Al Kα μ-focused monochromatic source (1486.6 eV) in K-alpha (Thermo Scientific Inc., U.K). All represented values of the binding energies in the paper are calibrated by adjusting binding energy of C 1s at 284.5 eV. The cryogenic H_2-temperature programmed reduction (cryo H_2-TPR) was conducted with a BEL-CAT-II (BEL Japan Inc.) with a thermal conductivity detector (TCD). Before analysis, 0.05 g of samples were pre-treated in a flow of N_2 at 120 °C for 2 h to eliminate water and other contaminants inside the sample. Subsequently, the samples were exposed to 5 vol% H_2/Ar and heated from −90 to 800 °C with the ramping rate of 10 °C min^{-1}. The Pd and Ni K-edge X-ray absorption spectroscopy (XAS) was performed at Pohang Accelerator Laboratory (7D-XAFS beamline in PLS-II) using Si (111) crystal as monochromator with the 2.5 GeV beam energy and 360 mA ring current. Energy calibration was carried out with Pd and Ni foils (24 350 eV and 8333 eV, respectively). Ionization chamber for incident and transmitted beam were purged with 1 atm of He and N_2, respectively. The step and duration time for X-ray absorption near edge structure (XANES) were 1 eV and 2 s, and 0.4 eV and 2 s for Pd and Ni, respectively.

Results and discussion

The catalytic activities for FAD reaction were measured with 10 mL formic acid (1 M) at 60 °C over differently prepared Ni-promoted Pd/C catalysts. $Pd_1/NiO_x/C$ (seq) catalysts with different Ni/Pd molar ratios ($x = 0.9$, 1.3, 1.6 and 3.1) were tested to optimize the ratio of Ni/Pd. Furthermore, $Pd_1NiO_{1.3}/C$ (co) and $Pd_1/NiO_{1.3}/C$ (seq) were compared to investigate the effect of impregnation methods. Fig. 2(a) displays the volumes of generated gas during FAD reaction over the catalysts as a function of reaction time. The larger volumes of generated gas over the seq-impregnated $Pd_1/NiO_x/C$ catalysts than that over Pd/C show remarkable promoting effect of pre-impregnated Ni on Pd based catalyst for FAD reaction. Interestingly, contrary to the high activity of $Pd_1/NiO_{1.3}/C$ (seq), when the co-impregnated catalyst was prepared with the same Ni/Pd ratio, the activity of $Pd_1NiO_{1.3}/C$ (co) is almost same as that of Pd/C. Then, the initial activities of the catalysts are plotted as a function of the Ni/Pd molar ratio (x) in Fig. 2(b). The initial activities were calculated in the time range from 3 to 4 min to ensure the stabilization of reaction such as temperature equilibrium between water bath and FA solution. The volcanic plot verifies the significant dependence of catalytic activity on Ni/Pd ratio. In addition, it should be mentioned that the highest activity is obtained over $Pd_1/NiO_{1.3}/C$ (seq) without generating any CO gas, which means that there is no dehydration reaction of formic acid (Fig. S2†).

X-ray diffraction analysis (XRD) was carried out to investigate phases of the catalysts. All catalysts exhibit the characteristic peaks arising from metallic Pd at around 40.2°, 46.6°, 68.0° and 82.2°, whereas no peak corresponding to crystalline PdO phase is observed (Fig. S3†). The Pd (111) planes at around 40.2° in all bimetallic catalysts are slightly shifted to the higher degree in comparison with Pd/C, indicating the changes in the lattice parameter of Pd due to the presence of Ni. When it comes to the peak broadness, the Pd (111) peak is the broadest in $Pd_1/NiO_{1.3}/C$ (seq), while $Pd_1NiO_{1.3}/C$ (co) has the sharpest peak among the bimetallic catalysts. Since Scherrer equation implies that the broader XRD peak represents the smaller crystallite size, $Pd_1/NiO_{1.3}/C$ (seq) and $Pd_1NiO_{1.3}/C$ (co) have the smallest and largest Pd crystallite size among the bimetallic catalysts,
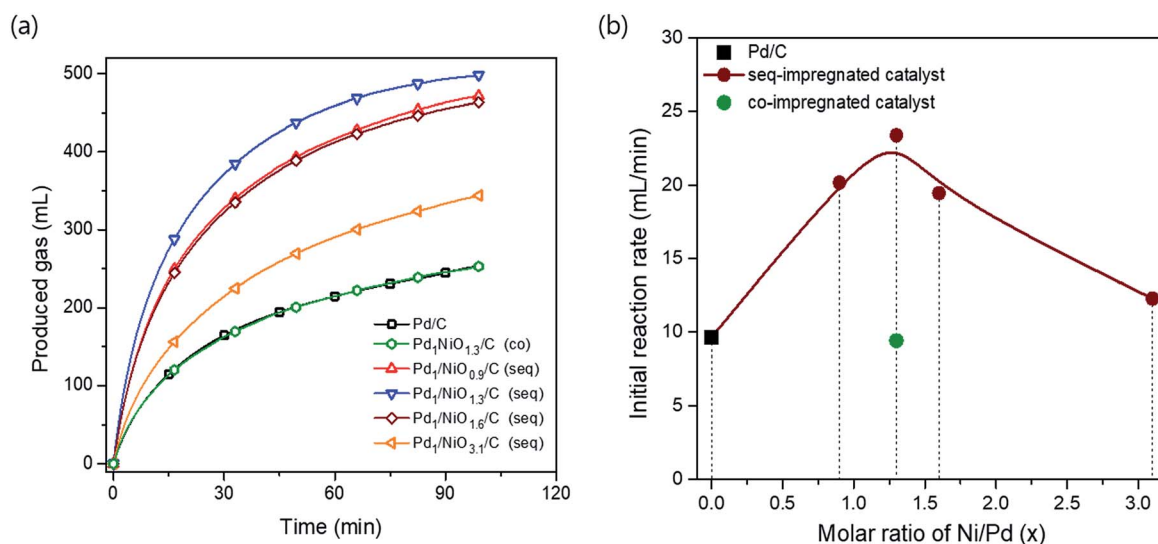

Fig. 2 (a) Volumes of produced gas over the 0.05 g of various Pd−Ni bimetallic catalysts during the reaction of 10 mL formic acid (1 M) at 60 °C and (b) their initial rates after stabilization (from 3 to 4 min) depending on the molar ratio of Ni/Pd (x).

respectively. Depending on Ni/Pd molar ratio (x) of seq-impregnated catalysts, the broadness of the Pd (111) peak becomes narrower when the ratio is larger or smaller than 1.3, indicating that the crystallite size of Pd is volcanically minimized at $x = 1.3$. Such trend of Pd crystallite size is consistent with that of average particle sizes obtained from transmission electron microscope (TEM) images represented in Fig. 3 and Table 1. It also demonstrates that the average particle sizes of seq-impregnated catalysts show the volcanic trend with the smallest particle size when the molar ratio of Ni/Pd is in the range from 1.3 to 1.6. Moreover, EDS mapping images of $Pd_1/NiO_{1.3}/C$ (seq) and $Pd_1NiO_{1.3}/C$ (co) in Fig. 3(g) and (h) shows that Pd and Ni are well-dispersed in a particle in both cases and that their geometric structures are not much different. Although the TEM analysis cannot clearly differentiate Pd and Ni in a particle as shown in EDS mapping images, because the trend of Pd crystallite size shown in XRD pattern is matched well with that of the particle size obtained from TEM, the catalyst with the smaller particle might have the smaller Pd crystallite. According to the results, even though $Pd_1NiO_{1.3}/C$ (co) has comparably

larger particle size than all seq-impregnated catalysts, it has still smaller particle size than Pd/C. It indicates that the presence of Ni in co-impregnated catalyst restrains the growth of Pd nanoparticles as reported in previous research, which showed the higher catalytic activity over the catalyst with smaller particle size.[21] More meaningfully, it is identified that the pre-impregnated Ni in seq-impregnated catalyst plays more effective role in constraining the growth of Pd nanoparticles than co-impregnated Ni, resulting in considerably smaller particle sizes of seq-impregnated catalysts even compared to co-impregnated catalyst. Correlating the particle size with the catalytic activity, the catalyst with smaller particle size showed the higher FAD reaction rate. Therefore, such inhibiting effect of pre-impregnated Ni on particle growth is one of important roles to improve the FAD activity. Zhou and Lee demonstrated the different adsorption and desorption behaviors of intermediates on Pd depending on the particle size of Pd/C catalyst during FA oxidation reaction.[30] Considering the lots of similarities between FA oxidation and FAD reaction, the particle size Pd is also expected to influence the adsorption and desorption behaviors of intermediates during the FAD reaction. Moreover, in addition to the previous researches briefly announcing the particle size effect,[14,21,31] the concrete effect of the Pd particle size on the activity was recently identified by Li et al., Navlani-García et al. and Zhang et al.[32–34] By adopting cuboctahedron-shape model, they concluded that the enhanced interaction between positive Pd and negative charged intermediates (e.g. formate ion) due to the large portion of edge Pd in small particle size. Therefore, it is concluded that the small size of Pd induced by pre-impregnated Ni is one important factor to enhance the FAD catalytic activity.

The electronic states of metals in the catalysts were investigated by using X-ray photoelectron spectroscopy (XPS). Since Ni has no activity by itself for FAD reaction (Fig. S1†) and there is no big difference in Ni phase between the Ni-containing catalysts (Fig. S4†), only the results of Pd are focused. The Pd 3d spectra in various catalysts are represented in Fig. 4, and the peak values of Pd $3d_{5/2}$ are listed in Table 1. It is well known that the binding energy of metal can be shifted to the lower or higher values by electron donation from or to neighboring atom, respectively. In case of the co-impregnated catalyst, $Pd_1NiO_{1.3}/C$ (co) has considerably lower binding energy of Pd 3d (335.80 eV) than Pd/C (336.13 eV), which is in agreement with the previous observations.[35–37] The shift of Pd 3d binding energy to the lower adjacent Ni atom to Pd according to the d-band theory.[38] In contrast, all the seq-impregnated catalysts have higher Pd 3d binding energy than Pd/C. It indicates that Pd atoms of seq-impregnated catalysts interact with neighboring atoms such as oxygen which can withdraw electron from Pd. Such different electron transfers between Pd and neighboring atom originate from the different synthetic processes. Considering the synthetic process of the co-impregnated catalyst, Pd^{2+} and Ni^{2+} are simultaneously reduced on carbon. Thus, Pd and Ni might interact directly with each other, which induce electron transfer from Ni to Pd, resulting in the shift of Pd 3d binding energy of $Pd_1NiO_{1.3}/C$ (co) to lower value in XPS. On the other hand, in the case of seq-impregnation, the phase of Ni/C prior to the
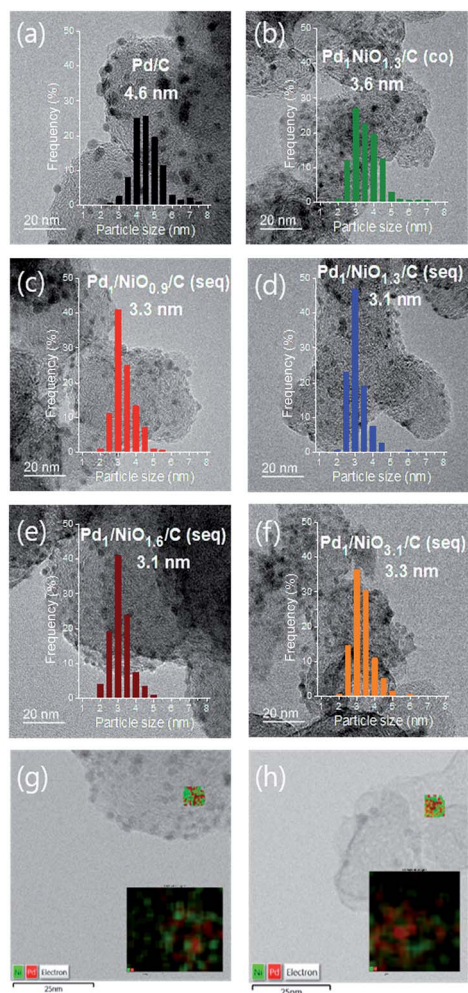

Fig. 3 TEM images and particle size distribution of (a) Pd/C, (b) $Pd_1NiO_{1.3}/C$ (co), (c) $Pd_1/NiO_{0.9}/C$ (seq), (d) $Pd_1/NiO_{1.3}/C$ (seq), (e) $Pd_1/NiO_{1.6}/C$ (seq) and (f) $Pd_1/NiO_{3.1}/C$ (seq); STEM and EDS mapping images of (g) $Pd_1/NiO_{1.3}/C$ (seq) and (h) $Pd_1NiO_{1.3}/C$ (co).

Table 1 The characterization information of Pd–NiO/C bimetallic catalysts obtained from ICP-AES, TEM image, cryo H_2-TPR and XPS analysis

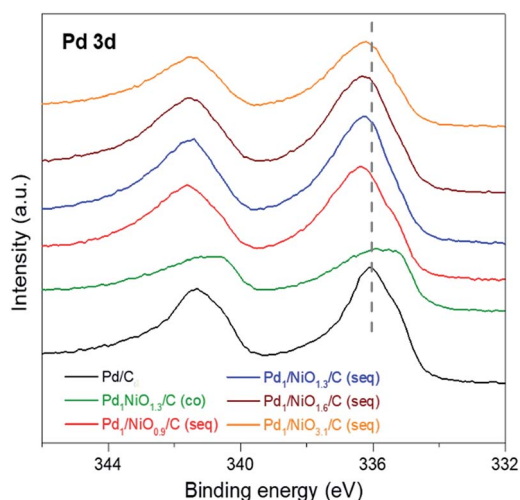|	wt%[a]		Averaged particle size[b] [nm]	The amount of Pd species			Binding energy of Pd $3d_{5/2}$[d] [eV]
	Pd	Ni		Total Pd[a] (mmol g^{-1})	Pd^{2+} species[c] (mmol g^{-1})	Pd^{2+} species/total Pd (mol%)	
Pd/C	8.7	—	4.6	0.818	0.402	49.2	336.13
$Pd_1NiO_{1.3}$/C (co)	9.1	6.6	3.6	0.855	0.276	32.2	335.80
Pd_1/$NiO_{0.9}$/C (seq)	8.9	4.2	3.3	0.836	0.698	83.5	336.32
Pd_1/$NiO_{1.3}$/C (seq)	8.8	6.2	3.1	0.827	0.773	93.5	336.32
Pd_1/$NiO_{1.6}$/C (seq)	9.0	7.9	3.1	0.846	0.726	85.8	336.31
Pd_1/$NiO_{3.1}$/C (seq)	9.4	15.8	3.3	0.883	0.345	39.2	336.15

[a] Obtained from ICP-AES. [b] Averaged by measuring more than 200 particles of TEM-images. [c] Calculated from hydrogen consumption and evolution from H_2-TPR. [d] Measured by XPS spectra.

impregnation of Pd is identified as NiO by the cryogenic hydrogen temperature programmed reduction (cryo H_2-TPR) (Fig. S5†). Even though Ni oxide can also be reduced by $NaBH_4$, the reduction of Pd^{2+} occurs much more rapidly than that of Ni oxide (Fig. S6†). Therefore, when Pd^{2+} is reduced on NiO/C, most of Pd^{2+} is prone to be impregnated on oxygen sites of Ni oxide due to high electronegativity of oxygen. Finally, Pd might interact with oxygen rather than Ni, as identified by the shift of Pd 3d binding energies of all seq-impregnated catalysts to higher values in XPS. The more positive Pd is known to interact better with negative charged intermediates such as formate ion during reaction, and moreover, Jia *et al.* suggested the formic acid decomposition pathway where formate ion acts as key intermediate.[39] The possible reaction pathway is as follows: (1) $HCOOH \leftrightarrow H^+ + HCO_2^-$, (2) $HCO_2^- + Pd \leftrightarrow PdH + CO_2 + e^-$, (3) $H^+ + Pd + e^- \leftrightarrow PdH$ and (4) $2PdH \leftrightarrow 2Pd + H_2$. Therefore, the high activity of seq-impregnated catalyst is attributed to the presence of electron-deficient Pd.[24,32–34] The XPS result can also explain the similar activity of $Pd_1NiO_{1.3}$/C (co) to Pd/C despite its smaller particle size than Pd/C. Because more negative Pd in $Pd_1NiO_{1.3}$/C (co) than Pd/C cannot interact well with negative charged intermediates, it counteracts the promoting effect of

small particle size of $Pd_1NiO_{1.3}$/C (co). Finally, as changes in electronic state of Pd vary the adsorption and desorption of intermediates, another reason for the enhanced activity of seq-impregnated catalysts is the electronic modification of Pd to be positive induced by the pre-impregnated Ni in addition to particle size effect.

The states of metals in Pd–NiO/C catalysts were analyzed by X-ray absorption near edge structure (XANES). The state of Pd in the samples varies as a function of impregnation method and Ni/Pd molar ratio as shown in Fig. 5. In detail, while the Pd state of Pd/C and $Pd_1NiO_{1.3}$/C (co) are similar to Pd metal, that of Pd_1/$NiO_{1.3}$/C (seq) is more close to PdO or $Pd(OH)_2$ reference than Pd metal. Furthermore, when molar ratio of Ni/Pd is larger or smaller than 1.3, the state of Pd becomes more metallic. The correlation between catalytic activity and the state of Pd clearly indicates that the catalyst having more oxidized Pd shows the higher catalytic activity. However, it should be recognized that such oxidized Pd in the catalysts cannot represent the phase of Pd during FAD reaction, since oxidized Pd is rapidly reduced to metallic Pd by a significant amount of H_2 produced from the FAD reaction at 60 °C in aqueous phase. The oxidation of Pd might occur during the drying process which was performed under air at the highest temperature (100 °C). Even though the temperature and time of oxidation condition can affect the extent of Pd oxidation, all the catalysts underwent the same synthetic process and were stabilized sufficiently in air at 100 °C. Therefore, the extent of oxidation is only determined by the property of Pd, which are affected by particle size and electronic property.

The quantitative analysis between the catalytic activity and the state of Pd is available with profiles of H_2-TPR in Fig. 6. The consumptions of H_2 at around 320 °C and 540 °C, which become larger as the Ni content increases, are assigned to the reduction of Ni oxide and hydrogenation of carbon to produce CH_4, respectively.[40,41] On the other hand, the α peak originates from H_2 consumption to reduce either PdO or $Pd(OH)_2$, and then to form Pd hydride (*i.e.* PdH_x). The β peak arises from H_2 evolution due to the thermal decomposition of PdH_x.[42,43] Since PdO can reversibly transform to $Pd(OH)_2$ in the presence of water and, moreover, their characteristic peaks in H_2-TPR are hardly differentiated similar to their XANES spectra (Fig. S5†),

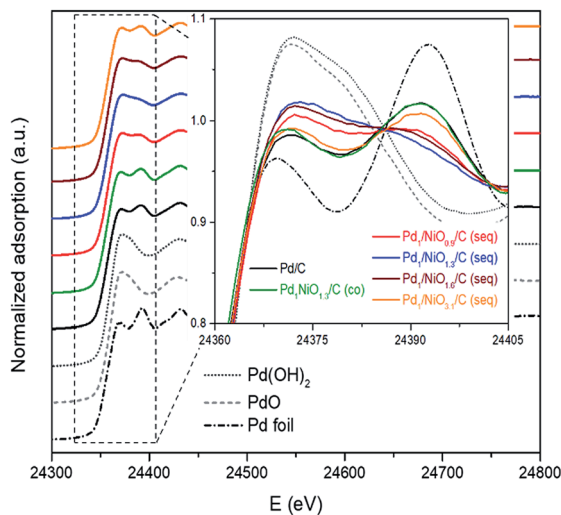**Fig. 4** XP spectra in Pd 3d region of various Pd–NiO/C catalysts.

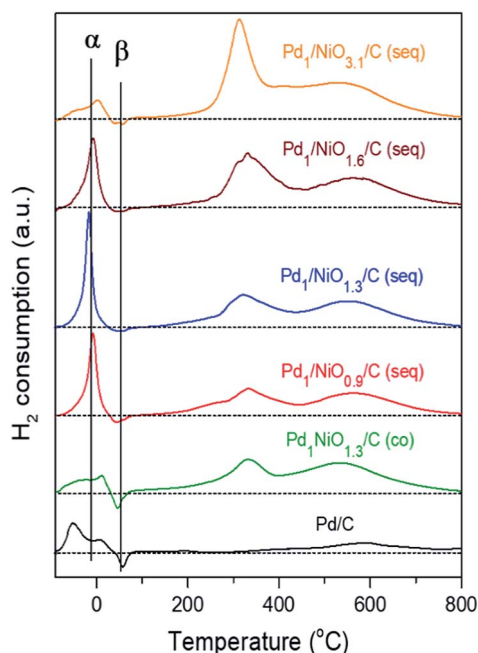Fig. 5 Normalized XANES spectra for Pd K-edges of Pd–NiO/C catalysts with references (*i.e.* Pd foil, PdO and Pd(OH)$_2$).

Fig. 6 Cryogenic H$_2$-TPR spectra of the various Pd–Ni catalysts obtained after drying.

catalyst makes Pd negative as identified by XPS analysis, the amount of Pd^{2+} species (0.276 mmol g^{-1}) of Pd$_1$NiO$_{1.3}$/C (co) is the lowest among the catalysts despite its smaller Pd size than Pd/C. In contrast, as the same ratio of Ni/Pd in seq-impregnated catalyst (*i.e.* Pd$_1$/NiO$_{1.3}$/C (seq)) promotes Pd to be positive and the smallest, it makes Pd form the largest amount of Pd^{2+} species (0.773 mmol g^{-1}).

When the molar percent of Pd^{2+} species obtained from H$_2$-TPR is correlated with the initial activity of the catalysts during the reaction, the positive linear correlation is clearly observed in Fig. 7. Previous researches have already been reported that the small and positive Pd species facilitates the adsorption of oxygen species like OH$_{ads}$ in aqueous phase as well as the removal of poisonous intermediate such as CO$_{ads}$.[30,46–48] Yoo *et al.* mapped TOF of H$_2$ and CO$_2$ production from FAD reaction as functions of adsorption energies of OH$_{ads}$ and CO$_{ads}$ through theoretical study.[48,49] According to their calculation, if Pd (111) plane binds more strongly to OH$_{ads}$ and less strongly to CO$_{ads}$ than theoretical values, the TOF over Pd (111) plane will be shifted to the highest TOF range of the volcanic curve. Their results can explain how the small and positive Pd can have the enhanced catalytic activity. Moreover, it is identified in previous paragraphs that the large amount of Pd^{2+} species is formed in the catalyst with the small particle size and electronically positive Pd. As small and positive Pd has the high catalytic activity and also forms the large amount of Pd^{2+} species, the content of Pd^{2+} species have positive linear correlation with catalytic activity. Thus, the content Pd^{2+} species can be used as quantitative index representing synergetic effect of particle size and electronic property which determine the catalytic activity.

The Pd$_1$/NiO$_{1.3}$/C (seq) catalyst was reused after the reaction, which was shown in Fig. 8(a). It was found that the reduced catalytic activity originated from loss of Ni metal after the reaction. Since the ionization tendency of Ni is larger than proton (H$^+$), the content of Ni in the catalyst decreased from 6.2 wt% to 0.5 wt% (ICP-AES) after the reaction while Pd almost
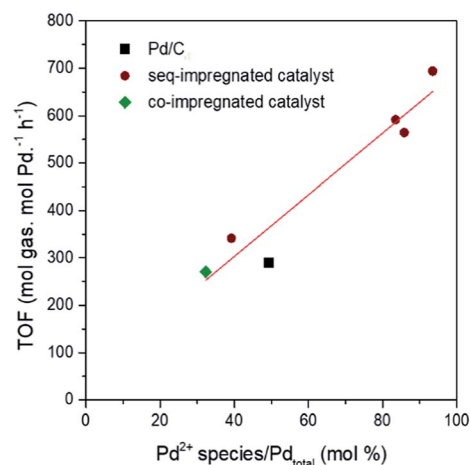
such indistinguishable species (*i.e.* PdO and Pd(OH)$_2$) are collectively named as Pd^{2+} species.[44,45] Regardless of PdO or Pd(OH)$_2$, as both Pd^{2+} species consumed equivalent amount of H$_2$ to be reduced to the metallic Pd, the collective amount of Pd^{2+} species in Table 1 could be obtained by subtracting the area of β peak from that of α peak, while total Pd (*i.e.* Pd^0 + Pd^{2+} species) content was attained from ICP analysis. In addition to electronic effect of promoter, as many other reports announced small Pd particle has more positive charge than large one, the smaller particle size of Pd can be more oxidized.[30,32,34,46] Since the presence of Ni (1.3 molar ratio of Ni/Pd) in co-impregnated

Fig. 7 The correlation between Pd^{2+} species/Pd$_{total}$ (mol%) and the TOF (mol gas mol Pd^{-1} h^{-1}) of the catalysts at early 1 min after stabilization (from 3 to 4 min) during the reaction of 10 mL formic acid (1 M) at 60 °C.
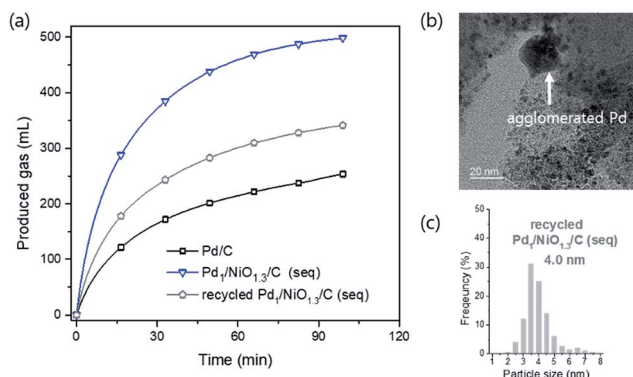
Fig. 8 (a) Catalytic activity test (10 mL 1 M formic acid at 60 °C) over recycled $Pd_1/NiO_{1.3}/C$ (seq) and its (b) TEM images and (c) particle size distribution with average particle size.

maintains its initial content at 8.9 wt%. In addition, some Pd particles were agglomerated and the average particle size was increased as shown in Fig. 8(b) and (c), resulting in the decrease of catalytic activity. It is possibly attributed to the reductive condition and the relatively high reaction temperature. Importantly, the content of Pd^{2+} species of recycled catalyst is right above the trend line in Fig. 7 (Fig. S7†). Thus, it supports our proposal that content of Pd^{2+} can be used as quantitative index.

Conclusions

In summary, current study allowed us to achieve the enhanced FAD activity of Pd–NiO/C catalyst, twice higher than that of Pd/C, by just applying the sequential impregnation method with the optimum molar ratio of Ni/Pd ($x = 1.3$). Despite limitation of commercial usage of Ni-promoted Pd/C catalyst due to the durability, the significance of our research lies in the investigation of the effect of sequential impregnation method on catalytic activity of FAD catalyst for the first time. It is noteworthy result that the property of Pd is largely dependent on the order of impregnation and the ratio of Ni/Pd. More importantly, these variables determine both the particle size and the electronic variation of Pd which are identified to play critical role in FAD reaction, because the smaller and more positive Pd species can facilitate the adsorption and desorption of intermediates during FAD reaction. As this study shows synergetic effects of particle size and electronic modification, it is expected to help developing advanced Pd-based catalyst *via* concrete direction which is to make smaller and more positive charged Pd by adopting proper promoter/support or preparation method.

Conflicts of interest

There are no conflicts to declare.

Acknowledgements

Notes and references

1 M. Höök and X. Tang, *Energy Policy*, 2013, **52**, 797–809.
2 P. P. Edwards, V. L. Kuznetsov, W. I. F. David and N. P. Brandon, *Energy Policy*, 2008, **36**, 4356–4362.
3 A. Sartbaeva, V. L. Kuznetsov, S. A. Wells and P. P. Edwards, *Energy Environ. Sci.*, 2008, **1**, 79–85.
4 G. J. Offer, D. Howey, M. Contestabile, R. Clague and N. P. Brandon, *Energy Policy*, 2010, **38**, 24–29.
5 M. A. Deluchi, *Int. J. Hydrogen Energy*, 1989, **14**, 81–130.
6 C. C. Elam, C. E. G. Padro, G. Sandrock, A. Luzzi, P. Lindblad and E. F. Hagen, *Int. J. Hydrogen Energy*, 2003, **28**, 601–607.
7 L. Schlapbach and A. Zuttel, *Nature*, 2001, **414**, 353–358.
8 S. S. Han, H. Furukawa, O. M. Yaghi and W. A. Goddard 3rd, *J. Am. Chem. Soc.*, 2008, **130**, 11580–11581.
9 J. Yang, A. Sudik, C. Wolverton and D. J. Siegel, *Chem. Soc. Rev.*, 2010, **39**, 656–675.
10 F. Joo, *ChemSusChem*, 2008, **1**, 805–808.
11 M. Grasemann and G. Laurenczy, *Energy Environ. Sci.*, 2012, **5**, 8171–8181.
12 D. Ruthven, *J. Catal.*, 1971, **21**, 39–47.
13 K. Tedsree, C. W. Chan, S. Jones, Q. Cuan, W. K. Li, X. Q. Gong and S. C. Tsang, *Science*, 2011, **332**, 224–228.
14 X. Zhou, Y. Huang, W. Xing, C. Liu, J. Liao and T. Lu, *Chem. Commun.*, 2008, 3540–3542, DOI: 10.1039/b803661f.
15 Y. Huang, X. Zhou, M. Yin, C. Liu and W. Xing, *Chem. Mater.*, 2010, **22**, 5122–5128.
16 R. Farrauto, S. Hwang, L. Shore, W. Ruettinger, J. Lampert, T. Giroux, Y. Liu and O. Ilinich, *Annu. Rev. Mater. Res.*, 2003, **33**, 1–27.
17 J. H. Lee, J. Ryu, J. Y. Kim, S. W. Nam, J. H. Han, T. H. Lim, S. Gautam, K. H. Chae and C. W. Yoon, *J. Mater. Chem. A*, 2014, **2**, 9490–9495.
18 H. M. Dai, B. Q. Xia, L. Wen, C. Du, J. Su, W. Luo and G. Z. Cheng, *Appl. Catal., B*, 2015, **165**, 57–62.
19 Y. Karatas, A. Bulut, M. Yurderi, I. E. Ertas, O. Alal, M. Gulcan, M. Celebi, H. Kivrak, M. Kaya and M. Zahmakiran, *Appl. Catal., B*, 2016, **180**, 586–595.
20 A. Bulut, M. Yurderi, Y. Karatas, Z. Say, H. Kivrak, M. Kaya, M. Gulcan, E. Ozensoy and M. Zahmakiran, *ACS Catal.*, 2015, **5**, 6099–6110.
21 Y. L. Qin, J. Wang, F. Z. Meng, L. M. Wang and X. B. Zhang, *Chem. Commun.*, 2013, **49**, 10028–10030.
22 M. Yurderi, A. Bulut, N. Caner, M. Celebi, M. Kaya and M. Zahmakiran, *Chem. Commun.*, 2015, **51**, 11417–11420.
23 S. Jones, A. Kolpin and S. C. E. Tsang, *Catal., Struct. React.*, 2014, **1**, 19–24.
24 L. Xu, F. Yao, J. Luo, C. Wan, M. Ye, P. Cui and Y. An, *RSC Adv.*, 2017, **7**, 4746–4752.
25 C. Feng, Y. H. Hao, L. Zhang, N. Z. Shang, S. T. Gao, Z. Wang and C. Wang, *RSC Adv.*, 2015, **5**, 39878–39883.
26 L. Xu, B. Jin, J. Zhang, D.-g. Cheng, F. Chen, Y. An, P. Cui and C. Wan, *RSC Adv.*, 2016, **6**, 46908–46914.

27 Y. L. Qin, Y. C. Liu, F. Liang and L. M. Wang, *ChemSusChem*, 2015, **8**, 260–263.

28 S. Zhang, O. Metin, D. Su and S. Sun, *Angew. Chem., Int. Ed. Engl.*, 2013, **52**, 3681–3684.

29 S. De, J. Zhang, R. Luque and N. Yan, *Energy Environ. Sci.*, 2016, **9**, 3314–3347.

30 W. J. Zhou and J. Y. Lee, *J. Phys. Chem. C*, 2008, **112**, 3789–3793.

31 Q.-L. Zhu, N. Tsumori and Q. Xu, *J. Am. Chem. Soc.*, 2015, **137**, 11743–11748.

32 J. Li, W. Chen, H. Zhao, X. Zheng, L. Wu, H. Pan, J. Zhu, Y. Chen and J. Lu, *J. Catal.*, 2017, **352**, 371–381.

33 M. Navlani-García, K. Mori, A. Nozaki, Y. Kuwahara and H. Yamashita, *ChemistrySelect*, 2016, **1**, 1879–1886.

34 S. Zhang, B. Jiang, K. Jiang and W. B. Cai, *ACS Appl. Mater. Interfaces*, 2017, **9**, 24678–24687.

35 A. K. Shukla, M. Neergat, P. Bera, V. Jayaram and M. S. Hegde, *J. Electroanal. Chem.*, 2001, **504**, 111–119.

36 M. A. Matin, J.-H. Jang and Y.-U. Kwon, *J. Power Sources*, 2014, **262**, 356–363.

37 S. Han, G. S. Chae and J. S. Lee, *Korean J. Chem. Eng.*, 2016, **33**, 1799–1804.

38 B. Hammer and J. K. Nørskov, *Adv. Catal.*, 2000, **45**, 71–129.

39 L. Jia, D. A. Bulushev, S. Beloshapkin and J. R. H. Ross, *Appl. Catal., B*, 2014, **160–161**, 35–43.

40 J. Zhang, F. Lu, W. Yu, J. Chen, S. Chen, J. Gao and J. Xu, *Catal. Today*, 2014, **234**, 107–112.

41 K. Fabicovicova, O. Malter, M. Lucas and P. Claus, *Green Chem.*, 2014, **16**, 3580–3588.

42 Q. W. Zhang, J. Li, X. X. Liu and Q. M. Zhu, *Appl. Catal., A*, 2000, **197**, 221–228.

43 T. C. Chang, J. J. Chen and C. T. Yeh, *J. Catal.*, 1985, **96**, 51–57.

44 C. F. Cullis, T. G. Nevell and D. L. Trimm, *J. Chem. Soc., Faraday Trans. 1*, 1972, **68**, 1406–1412.

45 F. H. Ribeiro, M. Chow and R. A. Dallabetta, *J. Catal.*, 1994, **146**, 537–544.

46 W. J. Zhou, M. Li, O. L. Ding, S. H. Chan, L. Zhang and Y. H. Xue, *Int. J. Hydrogen Energy*, 2014, **39**, 6433–6442.

47 M. R. Columbia and P. A. Thiel, *J. Electroanal. Chem.*, 1994, **369**, 1–14.

48 J. S. Yoo, F. Abild-Pedersen, J. K. Norskov and F. Studt, *ACS Catal.*, 2014, **4**, 1226–1233.

49 J. S. Yoo, Z. J. Zhao, J. K. Norskov and F. Studt, *ACS Catal.*, 2015, **5**, 6579–6586.